

Electronic Supplemental Information for

Directly bonded hybrid of graphene nanoplatelets and fullerene: facile solid-state mechanochemical synthesis and application as carbon-based electrocatalyst for oxygen reduction reaction

*Jian Guan, Xiang Chen, Tao Wei, Fupin Liu, Song Wang, Qing Yang, Yalin Lu, and Shangfeng Yang**

Hefei National Laboratory for Physical Sciences at Microscale, CAS Key Laboratory of Materials for Energy Conversion, Department of Materials Science and Engineering & Synergetic Innovation Center of Quantum Information & Quantum Physics, University of Science and Technology of China (USTC), Hefei 230026, China

Contents

- S1. Raman spectra of products with/without LiOH catalyst. [S2]**
- S2. O1s XPS spectrum of the graphene-C₆₀ hybrid. [S2]**
- S3. TGA curve of the graphene-C₆₀ hybrid in comparison with those of pristine graphite and C₆₀. [S3]**
- S4. Schematic illustration of the formation mechanism of the graphene-C₆₀ hybrid via ball-milling. [S3]**
- S5. Raman spectra of the products obtained with different catalysts. [S4]**
- S6. HR-TEM images of the graphene-C₆₀ hybrid taken at another site and the “blank” graphene nanoplatelets. [S4]**

S1. Raman spectra of products with/without LiOH catalyst.

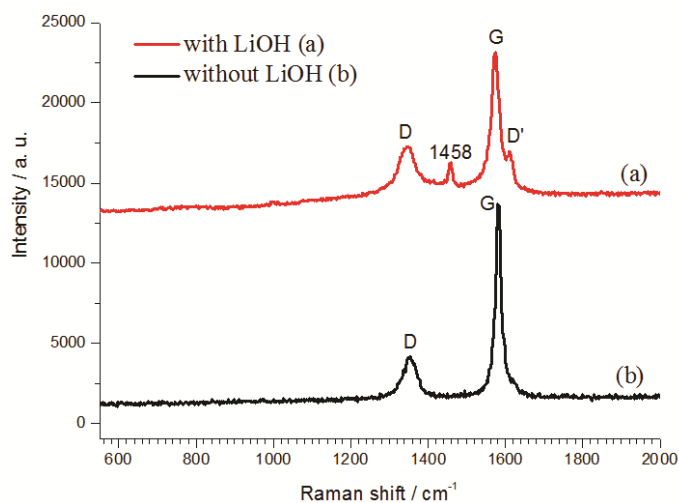


Figure S1. Raman spectra of products obtained from ball-milling of graphite and C₆₀ with LiOH catalyst (graphene-C₆₀ hybrid, curve a) and without LiOH catalyst (curve b).

Clearly, the characteristic Raman peak at 1458 cm⁻¹ assigned to C₆₀ in the Raman spectrum of the graphene-C₆₀ hybrid is not observed in the Raman spectrum of the product obtained from ball-milling of graphite and C₆₀ without LiOH catalyst, revealing that graphene-C₆₀ hybrid did not form in this case.

S2. O1s XPS spectrum of the graphene-C₆₀ hybrid.

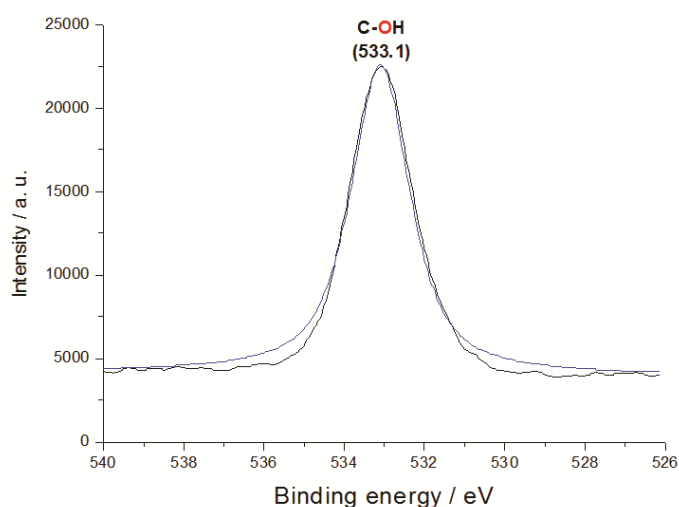


Figure S2. O1s XPS spectrum of the graphene-C₆₀ hybrid.

S3. TGA curve of the graphene-C₆₀ hybrid in comparison with those of pristine graphite and C₆₀.

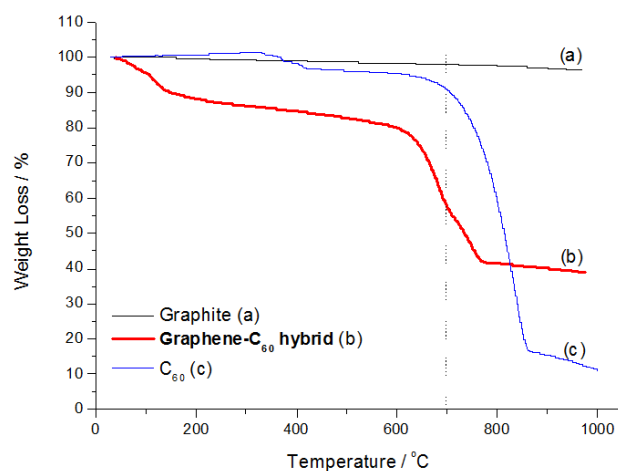
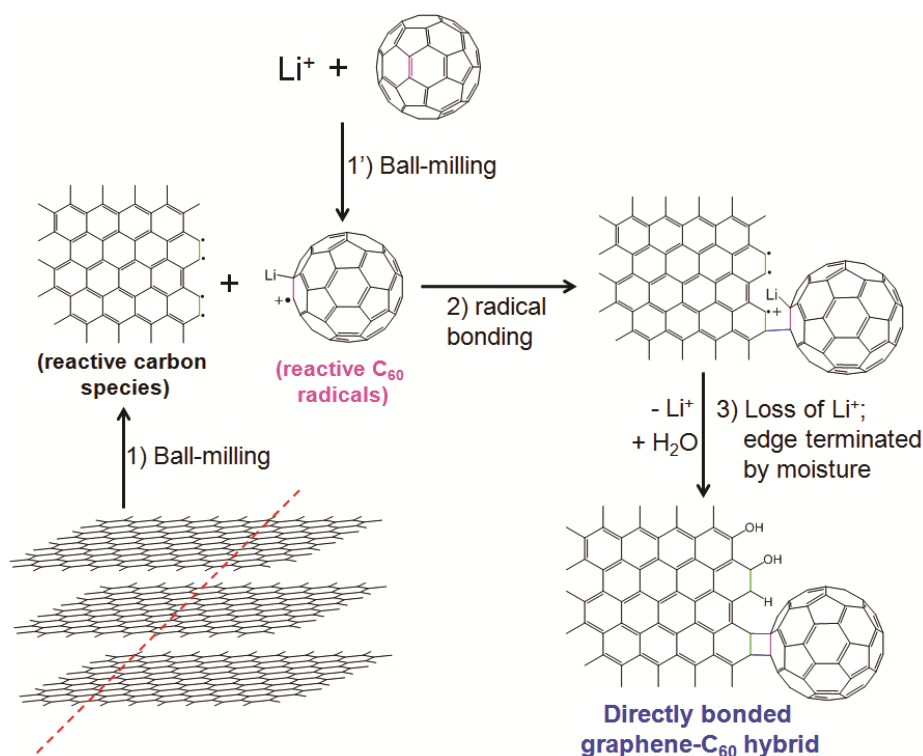


Figure S3. TGA curves of pristine graphite (a), the graphene-C₆₀ hybrid (b), and C₆₀ (c). A dotted vertical line was added to aid identifying the last step (700 - 770 °C) related to the decomposition of C₆₀.

S4. Schematic illustration of the formation mechanism of the graphene-C₆₀ hybrid via ball-milling.



Scheme S1. Schematic illustration of the formation mechanism of the graphene-C₆₀ hybrid via the mechanochemical ball-milling.

S5. Raman spectra of the products obtained with different catalysts.

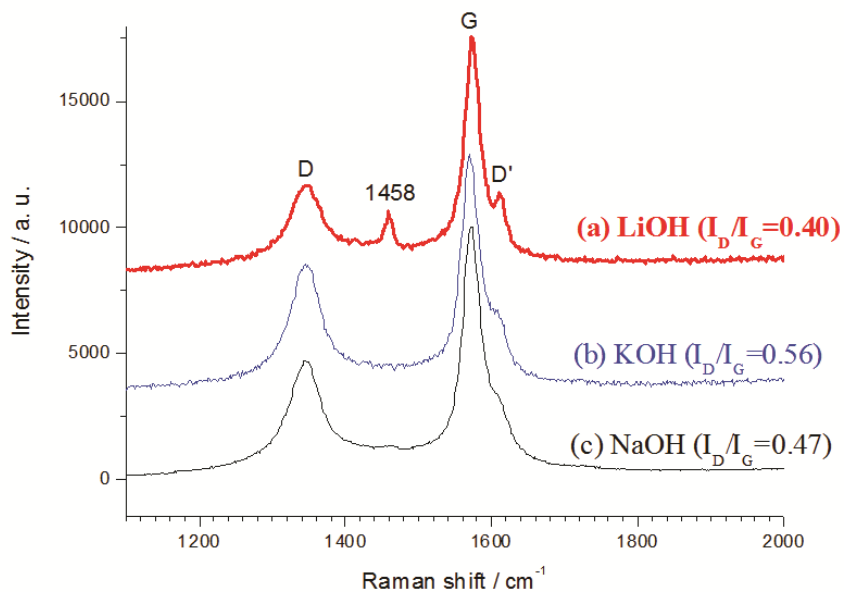


Figure S4. Raman spectra of the products obtained from ball-milling graphite and C₆₀ with different catalysts of LiOH (a), KOH (b) or NaOH (c).

S6. HR-TEM images of the graphene-C₆₀ hybrid taken at another site and the “blank” graphene nanoplatelets.

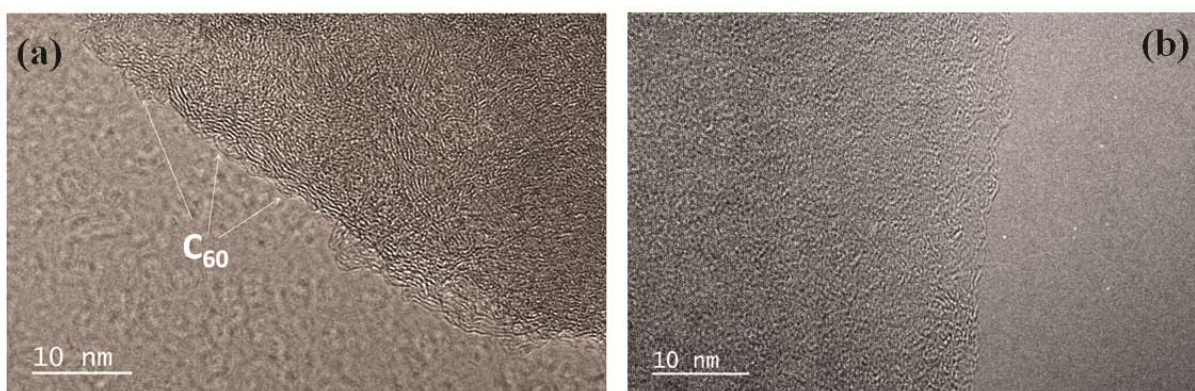


Figure S5. HR-TEM images of the graphene-C₆₀ hybrid taken at another site different to that shown in Figure 5 (a) and the “blank” graphene nanoplatelets prepared by ball-milling pure graphite under identical conditions (b).